

Transport of Long-Range Dependent Traffic in Single-Hop and Multi-Hop IEEE 802.11e Networks

Stefano Bregni, *Senior Member, IEEE*, Paolo Giacomazzi, Gabriella Saddemi

Politecnico di Milano, Dept. of Electronics and Information, Piazza Leonardo Da Vinci 32, 20133 Milano, ITALY
Tel.: +39-02-2399.3503 – Fax: +39-02-2399.3413 – E-mail: {[bregni](mailto:bregni@elet.polimi.it),[giacomaz](mailto:giacomaz@elet.polimi.it),[saddemi](mailto:saddemi@elet.polimi.it)}@elet.polimi.it

Abstract — Long-range dependence (LRD) is a widely verified property of traffic crossing the wireless LAN radio interface. LRD severely affects network performance yielding longer queuing delays. In this paper, we study how LRD and non-LRD traffic flows influence each other in the IEEE 802.11e wireless access network and their queuing behaviour in downstream schedulers. We consider scenarios with one and two wireless hops. We investigate interaction of traffic flows with the service class separation enabled by the IEEE 802.11e EDCA function, comparing results with those of the basic scenario with a single service class shared by all traffic flows. We find that a partial isolation of service classes is enabled by the IEEE 802.11e access function. However, competing flows exhibit a queuing behavior, in downstream schedulers, which cannot be accounted for by standard LRD traffic descriptors.

Index Terms — Communication system traffic, long-range dependence, quality of service, queuing analysis, traffic control (communication), wireless LAN.

I. INTRODUCTION

Many recent studies [1]-[5] have demonstrated the widespread presence of Self-Similarity (SS) and Long-Range Dependence (LRD) in LAN and WAN traffic. These properties affect severely network performance, yielding longer queuing delays [6]-[11]. In a SS random process, a dilated portion of a realization, by the scaling Hurst parameter H , has same statistical characterization as the whole. On the other hand, LRD is a long-memory property, usually equated to an asymptotic power-law decrease of the power spectral density (PSD) or, equivalently, of the autocovariance function [10].

Also wireless LAN (WLAN) traffic exhibits SS and LRD [1][10][12]. LRD properties of IEEE 802.11b WLAN traffic have been studied empirically in [13]. The authors concluded that LRD is present in IEEE 802.11b WLAN traffic at all levels of traffic load, but higher degree of LRD is present under higher traffic load. Liang [14] exploited the SS properties found in a real ad-hoc network for traffic forecasting. Yu and Petropolu [15] studied the propagation of SS of traffic through wireless, energy-conserving gateways. Tickoo and Sikdar [16] developed an analytical model of the interarrival time distribution in IEEE 802.11 networks, detecting a clustering effect of interarrival times around some values. They presented simulations and argued that aggregated traffic at the output of the IEEE 802.11 nodes seems to follow a multifractal model.

In [17], the authors describe the influence of medium access control (MAC) mechanisms and propagation impairments on the traffic characteristics, when LRD traffic traverses IEEE

802.11 links. This issue is relevant, as the traffic shaping performed by 802.11 access nodes may influence the performance of backbone networks. The most significant phenomena registered in [17] are the smoothing effect of the MAC mechanisms on the traffic at highest frequencies, while at lowest frequencies the authors found a SS mitigation that seems to be caused by packet loss induced by propagation impairments.

Recently, the possibility of managing differentiated QoS levels in WLAN has been introduced by the IEEE 802.11e standard [18]. The (partial) isolation of service classes in IEEE 802.11e access networks may allow to mitigate the strong mutual influence between traffic flows competing for radio resources and could prevent, at least partially, LRD traffic to affect the QoS of other traffic flows with shorter autocorrelation. However, at least to our knowledge, there are no works in literature studying the behavior of LRD traffic in IEEE 802.11e networks, neither in single-hop nor in multi-hop scenarios.

In this paper, we study the influence of MAC mechanisms on characteristics of LRD traffic traversing IEEE 802.11e links. We study several scenarios by simulation, by comparing the statistical properties of input traffic with those at the output of the wireless network segment. We analyze the statistical properties of traffic flows crossing the WLAN interface in single-hop and multi-hop scenarios, with and without the service class separation allowed by the IEEE 802.11e access mechanism. In particular, we study the α LRD-parameter of traffic, which describes the asymptotic behavior of the power spectral density of LRD traffic for $f \rightarrow 0$. Then, we study the queuing performance of traffic flows in downstream schedulers, after mutual interaction at the radio interface. We find that the queuing behavior of flows after the crossing of the WLAN network cannot be described by means of standard LRD indices such as α .

II. PRINCIPLES OF IEEE 802.11E EDCA

The IEEE 802.11e Enhanced Distributed Channel Access (EDCA) has been standardized in order to support prioritized services in the IEEE 802.11 Distributed Coordination Function (DCF), which only provides best-effort services in its current form. In EDCA, there are four Access Categories (ACs) to implement prioritized services. Each AC transmits packets with an independent channel access function, characterized by different values of both collision window and backoff timer.

Before starting transmission, each AC executes an independent backoff process to determine the transmission time of its

frame. The backoff process is regulated by four configurable parameters: CW_{min} , CW_{max} , $AIFS$ and $TXOP\ limit$. Specifically, for the i^{th} Access Category, with $i \in \{0, 1, 2, 3\}$, the initial backoff window size is $CW_{min,i}$, the maximum backoff window size is $CW_{max,i}$, and the arbitration inter-frame space is $AIFS_i$. For $0 \leq i < j \leq 3$, $CW_{min,i} \geq CW_{min,j}$, $CW_{max,i} \geq CW_{max,j}$, and $AIFS_i \geq AIFS_j$. Thus, the AC with higher index has higher priority, having higher probability to gain channel access.

When a station needs to transmit a new AC_i frame, it monitors channel activity and, if the channel is idle for a time period equal to its arbitration interframe space ($AIFS_i$), the frame is transmitted. Otherwise, if the channel is sensed busy (either immediately or during the $AIFS_i$ period), the channel is monitored until sensed idle for an $AIFS_i$ time. Then, the backoff process is started by initializing the backoff time counter to a random value uniformly distributed in range $(0, CW_i - 1)$, where CW_i is the collision window of AC_i and depends on the number of failed transmissions.

At the first transmission attempt, CW_i is set equal to the minimum collision window parameter ($CW_{min,i}$). As long as the channel is sensed idle, the backoff time counter is decremented once every time slot, where the slot time duration is a constant defined by the physical layer. When a transmission is detected on the channel, the backoff time counter is blocked and it is reactivated when the channel is sensed idle for an $AIFS_i$, if the transmission is successfully received. As soon as the backoff time counter reaches zero, the frame is transmitted in the next slot time. A collision occurs when two or more transmissions start simultaneously.

An acknowledgment (ACK) frame is used to notify the transmitting station that the frame has been successfully received. The ACK is transmitted at the end of the frame after a period of time equal to the physical layer constant short inter-frame space (SIFS). If the ACK is not received within a specified ACK timeout, the transmitted frame is assumed lost and a retransmission is scheduled by restarting the backoff process. After each unsuccessful transmission, CW_i is doubled up to a maximum value given by $CW_{max,i}$. To reduce collisions caused by hidden terminals and improve channel efficiency for long data transmissions, the request to send/clear to send (RTS/CTS) mechanism is used. Thus, a four-way RTS/CTS/DATA/ACK handshake is used for frame transmission.

III. SELF-SIMILARITY AND LONG-RANGE DEPENDENCE

A random process $X(t)$ (e.g., cumulative packet arrivals in time interval $[0, t]$), is said to be *self-similar*, with scaling parameter of self-similarity or Hurst parameter $H > 0$, $H \in \mathfrak{R}$, if

$$X(t) =_d a^{-H} X(at) \quad (1)$$

for any $a > 0$, where $=_d$ denotes equality for all finite-dimensional distributions [10]. In other terms, the statistical description of $X(t)$ does not change by *scaling* its amplitude by a^{-H} and its time by a . Most SS processes are not stationary.

The class of SS processes is usually restricted to that of *self-similar processes with stationary increments* (SSSI), which are “integral” of some stationary process. For example, consider the δ -increment process of $X(t)$, defined as $Y_\delta(t) = X(t) - X(t - \delta)$

(e.g., packet arrivals in the last δ time units). For a SSSI process $X(t)$, $Y_\delta(t)$ is stationary and $0 < H < 1$ [10].

Long-range dependence of a process is defined by an asymptotic power-law decrease of its autocovariance and PSD [10]. Let $Y(t)$ be a 2nd-order stationary random process. $Y(t)$ exhibits LRD if its autocovariance follows asymptotically

$$R_Y(\tau) \sim c_1 |\tau|^{\alpha-1} \quad \text{for } \tau \rightarrow +\infty, 0 < \alpha < 1 \quad (2)$$

or, equivalently, its two-sided PSD follows asymptotically

$$S_Y(f) \sim c_2 |f|^{-\alpha} \quad \text{for } f \rightarrow 0, 0 < \alpha < 1 \quad (3).$$

In general, a random process with non-integer power-law PSD is also known as fractional (not necessarily Gaussian) noise. It can be proven [10] that H-SSSI processes $X(t)$ with $1/2 < H < 1$ have LRD increments $Y(t)$, with

$$\alpha = 2H - 1 \quad (4).$$

IV. SCENARIOS FOR PERFORMANCE EVALUATION

We selected two scenarios for performance evaluation. In scenario 1 (Fig. 1), the wireless IEEE 802.11e network comprises one wireless cell including two traffic sources (S1, S0) and a router R1 providing the connection to the fixed network. The traffic flows from S1 and S0 are denoted $x_1(t)$ and $x_0(t)$, respectively. Traffic flows $x_1(t)$ and $x_0(t)$ compete according to the IEEE 802.11e EDCA mechanisms to reach the router R1.

Flows $x_1(t)$ and $x_0(t)$ may either belong to the same service class (*same-class* scenario) or be assigned to two different service classes (*different-class* scenario). In the same-class scenario, both $x_1(t)$ and $x_0(t)$ are served in class 0. In the different-class scenario, $x_1(t)$ is assigned to class 1 and $x_0(t)$ to class 0.

Packets originally generated by S1 (S0) form the traffic process $y_1(t)$ ($y_0(t)$) at the input of router R1. R1 is assumed to treat $y_1(t)$ and $y_0(t)$ with a rate-based scheduler assigning a dedicated and constant service capacity C_1 and C_0 to $y_1(t)$ and $y_0(t)$, respectively. In this way, $y_1(t)$ and $y_0(t)$ do not interfere in R1 and their queuing behaviour can be studied separately. From a practical standpoint, this assumption could model a scenario where $y_1(t)$ and $y_0(t)$ follow different paths from R1.

In scenario 2 (Fig. 2), two wireless hops are provided by the wireless router N1. The assumptions made for scenario 1 apply also here. In this case, we denote as $y_1(t)$ and $y_0(t)$ the traffic flows, originally generated by S1 and S0, at R1 input.

In conclusion, we defined four scenarios:

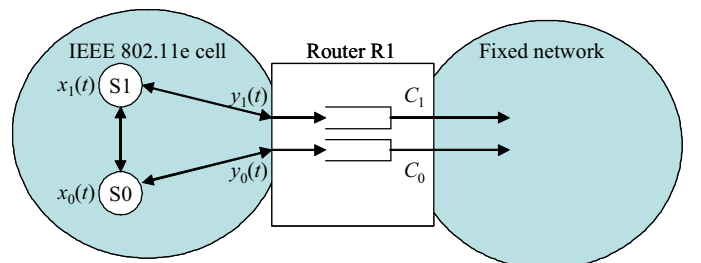


Fig. 1: Scenario 1 - one-hop wireless network.

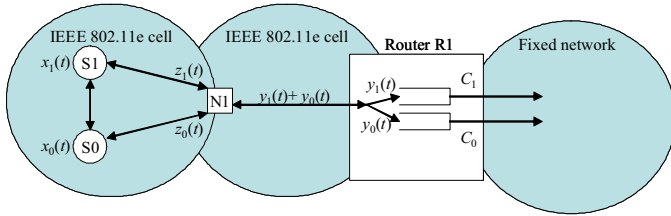


Fig. 2: Scenario 2 - two-hops wireless network.

Table 1: IEEE 802.11 system parameters.

Bit rate for data packets	Scenario 1 hop: 9 Mbit/s Scenario 2 hops: 24 Mbit/s
Bit rate for RTS/CTS/ACK	6 Mbit/s
PLC data rate	6 Mbit/s
Backoff Slot Time (ST)	9 μ s
SIFS	16 μ s
DIFS	34 μ s
PHY header	192 bits
MAC header	224 bits
IP header	160 bits
DATA packet	L payload bits + PHY header + MAC header + IP header
RTS	160 bits + PHY header
CTS, ACK	112 bits + PHY header

Table 2: QoS parameters for traffic sources.

Scenarios 1 e 2			
Traffic	AIFS (μ s)	CW_{min} (ST)	CW_{max} (ST)
Class 1 sources	34	3	7
Class 0 sources	43	7	15

- scenario 1 (one hop), same class;
- scenario 1 (one hop), different classes;
- scenario 2 (two hops), same class;
- scenario 2 (two hops), different classes.

For all scenarios, we will examine the characteristics of the $y_1(t)$ and $y_0(t)$ traffic processes and their queuing behaviour in the scheduler of the fixed network router R1.

As far as the LRD traffic model is concerned, in this paper we focus on fractional Gaussian traffic (fGt), being this model commonly adopted in literature. Our procedure of traffic synthesis, detailed in [19], generates LRD pseudorandom sequences $\{x_k\}$ of traffic fGt_R(α, m_x, σ_x^2), with PSD $\propto 1/f^\alpha$ for assigned values of α with $0 \leq \alpha < 1$, normally-distributed samples, mean m_x and variance σ_x^2 , rectified to avoid negative samples. The sequence $\{x_k\}$ represents the incremental data count [bit/s] at each time unit (i.e., the input traffic rate).

For estimating accurately the α parameter of LRD traffic series, we used the Modified Allan Variance (MAVAR) [19]. MAVAR is a well-known time-domain quantity, conceived in 1981 for frequency stability characterization of precision oscillators [21]–[24] by modifying the definition of the original Allan Variance. MAVAR was proven to feature superior spectral sensitivity and accuracy in LRD parameter estimation, coupled with excellent robustness against data nonstationarity (e.g., drift and steps) [19].

V. SIMULATION RESULTS

We evaluated the system performance by means of a simulator built using the TKN implementation of 802.11e EDCA for ns-2 [[25]. The parameter settings are outlined in Table 1. The only difference between scenarios 1 and 2 is the bit rate for data packets, equal to 9 Mbit/s in for one hop and 24 Mbit/s for two hops. We selected these values of data rate in order to guarantee that in both scenarios the service capacity at each wireless hop is larger than the average aggregate gross data rate (i.e. including overheads) on the air interface. This way, we avoid long-term congestions of the wireless network, while we allow short-term congestions (manageable with standard buffering) due to variable input traffic.

The IEEE 802.11e EDCA QoS parameters for service classes 1 and 0 are outlined in Table 2. We separated the collision windows of the two service classes in order to minimize their mutual interference across the radio interface.

Both $x_1(t)$ and $x_0(t)$ are fGt_R series made of $N = 2^{18}$ samples. For both sequences, we set the time unit $\tau_0 = 1$ ms, the mean $m_x = 2279$ bit per time unit (i.e., 2.279 Mbit/s) and the deviation $\sigma_x = 773.9$ bit per time unit (i.e., 773.9 kbit/s), as in [26]. At each time unit, a packet payload is generated and a packet ready for transmission is inserted in the transmission buffer of the source, by adding to the payload the protocol overheads specified in Table 1. The capacity assigned to classes 1 and 0 in the fixed network router R1 are $C_1 = C_0 = 2.848$ Mbit/s, to have load of schedulers serving $y_1(t)$ and $y_0(t)$ equal to 80%.

We run extensive simulations to characterize flows $y_1(t)$ and $y_0(t)$ at the interface between wireless and wired networks. Sources generate traffic for 2^{18} time units, feeding transmission buffers served according to the IEEE 802.11e EDCA rules. When sources stop generating traffic, the transmission buffers flush the stored content and the simulation is stopped.

In Figs. 3 through 10, we plot the parameters $\alpha_{OUT,1}$ and $\alpha_{OUT,0}$ estimated by MAVAR respectively on $y_1(t)$ and $y_0(t)$, as a function of the parameters $\alpha_{IN,1}$ and $\alpha_{IN,0}$ of the input traffic flows $x_1(t)$ and $x_0(t)$, in the four scenarios. The average slope of MAVAR curves was estimated excluding the first and last decade of τ values [19].

Figs. 3 and 4 show that in the one-hop scenario, when the two traffic flows share the same service class, both $\alpha_{OUT,1}$ and $\alpha_{OUT,0}$ can take very different values from the respective values of $\alpha_{IN,1}$ and $\alpha_{IN,0}$. The difference can be substantial: for example, with $\alpha_{IN,1} = 0$ and $\alpha_{IN,0} = 0.8$, we have $\alpha_{OUT,1} = 0.01$ and $\alpha_{OUT,0} = 0.6$. The variation of the α of $x_0(t)$ is significant, while the variation of the α of $x_1(t)$ is small. With two wireless hops (Fig. 7 and 8) and the same parameters of input traffic, we have measured $\alpha_{OUT,1} = 0.39$ and $\alpha_{OUT,0} = 0.38$. In this case both $\alpha_{OUT,1}$ and $\alpha_{OUT,0}$ change significantly.

By assigning the two traffic flows to different service classes, we obtain a significant isolation of flow LRDs. Figs. 5 and 6 plot $\alpha_{OUT,1}$ and $\alpha_{OUT,0}$ as a function of $\alpha_{IN,1}$ and $\alpha_{IN,0}$ in the one-hop scenario, by carrying traffic flow $x_1(t)$ in service category 1 and $x_0(t)$ in service category 0. Each traffic flow keeps its α parameter: that is, $\alpha_{OUT,1} \sim \alpha_{IN,1}$ and $\alpha_{OUT,0} \sim \alpha_{IN,0}$.

However, the same does not hold for the two-hops scenario

(Figs. 9 and 10), where the higher-priority traffic flow keeps its α parameter ($\alpha_{OUT,1} \sim \alpha_{IN,1}$) while the lower-priority flow experiences a significant distortion of the $\alpha_{OUT,0}$ parameter, which is heavily influenced by $\alpha_{IN,1}$ (i.e., we observe cross-service class interference). In particular (Fig. 10), $\alpha_{OUT,0}$ grows as $\alpha_{IN,1}$ increases (with $\alpha_{IN,0} = 0$ and $\alpha_{IN,1} = 0.8$, we have $\alpha_{OUT,0} = 0.52$). Even if the input traffic process $x_0(t)$ is white, $y_0(t)$ acquires a LRD feature if $x_1(t)$ has a strong correlation.

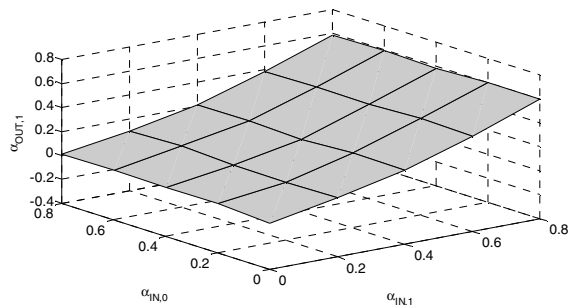


Fig. 3: Scenario 1, same class, $\alpha_{OUT,1}$.

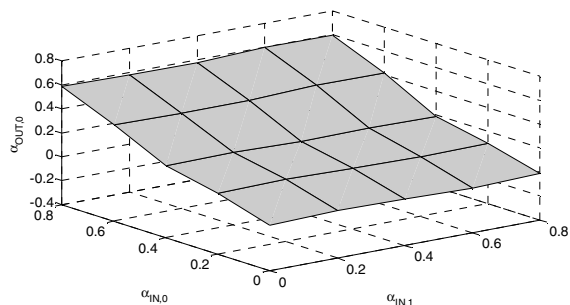


Fig. 4: Scenario 1, same class, $\alpha_{OUT,0}$.

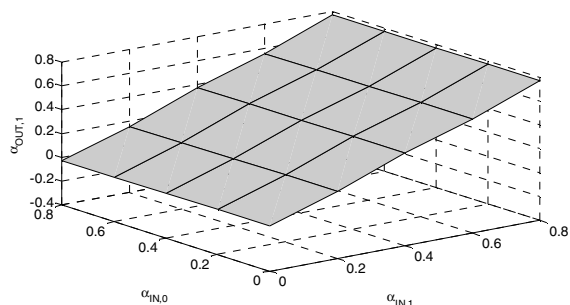


Fig. 5: Scenario 1, different class, $\alpha_{OUT,1}$.

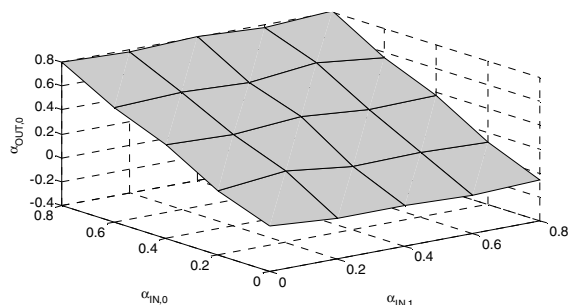


Fig. 6: Scenario 1, different class, $\alpha_{OUT,0}$.

Then, we studied the delay performance of traffic flows $y_0(t)$ and $y_1(t)$ in the schedulers of router R1, with $\alpha_{IN,0} = 0.8$,

$\alpha_{IN,1} = 0$ and $\alpha_{IN,0} = 0$, $\alpha_{IN,1} = 0.8$, in order to investigate the effects of the interaction of a white with a strongly correlated flow, when the white flow has both higher and lower priority than the correlated flow in the wireless segment of the end-to-end path. In order to correlate easily the queuing behavior of $y_1(t)$ and $y_0(t)$ with the respective values of α , we reported in Table 3 the values of $\alpha_{OUT,1}$ and $\alpha_{OUT,0}$ in the selected cases.

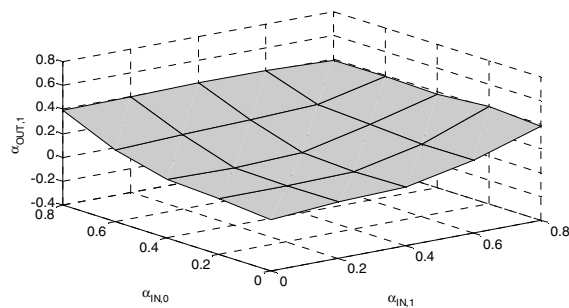


Fig. 7: Scenario 2, same class, $\alpha_{OUT,1}$.

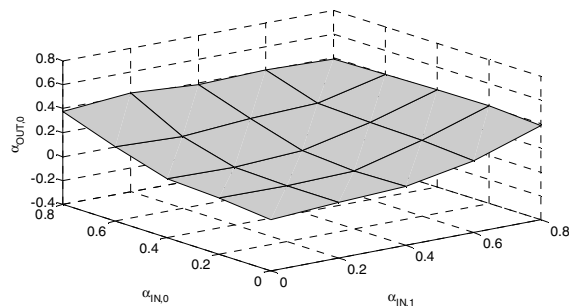


Fig. 8: Scenario 2, same class, $\alpha_{OUT,0}$.

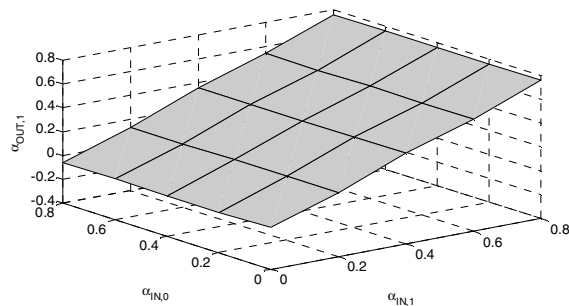


Fig. 9: Scenario 2, different class, $\alpha_{OUT,1}$.

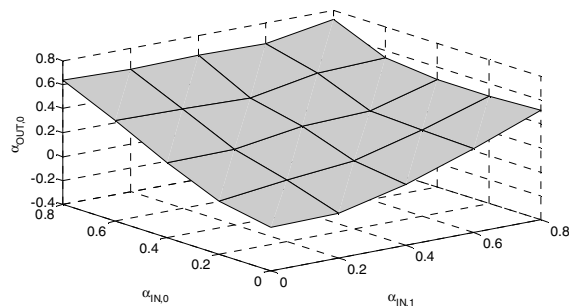


Fig. 10: Scenario 2, different class, $\alpha_{OUT,0}$.

In Figs. 11 and 12, we plotted the complementary distribution function of the delay experienced by flows $y_1(t)$ and $y_0(t)$ in the fixed network router R1 for $\alpha_{IN,0} = 0.8$, $\alpha_{IN,1} = 0$ and

$\alpha_{IN,0} = 0$, $\alpha_{IN,1} = 0.8$, respectively. For comparison, in these graphs we also plotted the distribution of the delay that would be experimented by flows $x_1(t)$ and $x_0(t)$ if they were fed directly into the schedulers of router R1. In this way, we are able to compare the delay tails of a traffic flow crossing one or two IEEE 802.11e wireless hops with the delay tail that would be experienced by the fresh input traffic in the same scheduler.

Table 3: values of $\alpha_{OUT,1}$ and $\alpha_{OUT,0}$ in the selected scenarios.

$\alpha_{IN,0} = 0.8, \alpha_{IN,1} = 0$ (Fig. 11)		
	One hop	Two hops
Same class	$\alpha_{OUT,1} = 0.01$	$\alpha_{OUT,1} = 0.39$
	$\alpha_{OUT,0} = 0.6$	$\alpha_{OUT,0} = 0.38$
Different class	$\alpha_{OUT,1} = -0.03$	$\alpha_{OUT,1} = -0.06$
	$\alpha_{OUT,0} = 0.8$	$\alpha_{OUT,0} = 0.64$
$\alpha_{IN,0} = 0, \alpha_{IN,1} = 0.8$ (Fig. 12)		
	One hop	Two hops
Same class	$\alpha_{OUT,1} = 0.6$	$\alpha_{OUT,1} = 0.39$
	$\alpha_{OUT,0} = -0.01$	$\alpha_{OUT,0} = 0.39$
Different class	$\alpha_{OUT,1} = 0.77$	$\alpha_{OUT,1} = 0.76$
	$\alpha_{OUT,0} = -0.06$	$\alpha_{OUT,0} = 0.52$

Since both $x_1(t)$ and $x_0(t)$ are fractional Gaussian traffic, their delay tail in the schedulers of router R1 are Weibull distributed, i.e. the queuing delay D exceeds a given threshold d with asymptotic probability $P\{D > d\} \sim \exp(-\beta d^{1-\alpha})$, where β is a positive function of the α parameter and of other network parameters. Note that with $\alpha=0$ (white traffic) the Weibull delay tail is exponential. The Weibull queue length distribution departs significantly from the exponential distribution resulting with white input traffic. In particular, the closer α is to 1, the slower the queue distribution decreases, making higher the queuing delay. Therefore, for fresh fGt traffic, the network delay performance depends considerably on actual values of the α parameter, among others.

Given the primary role of α in determining the queuing behaviour of LRD traffic, we would expect that in the schedulers of R1 the delay tail of $y_1(t)$ and $y_0(t)$ are strictly related to the values of $\alpha_{OUT,1}$ and $\alpha_{OUT,0}$ (Table 3). However, Figs. 11 and 12 contradict this conjecture. In these graphs: 1) solid curves refer to $x_0(t)$ and $y_0(t)$ and dotted curves refer to $x_1(t)$ and $y_1(t)$; 2) thin lines refer to the one-hop scenario, while thick lines to two-hops; 3) the square marker indicates the same class scenario, while the rhombus indicates different classes.

With reference to Fig. 11 ($\alpha_{IN,0} = 0.8$, $\alpha_{IN,1} = 0$), let us consider first the one-hop scenario with same class. Flow $y_1(t)$ has delay distribution with longer tail than that of $x_1(t)$: i.e., by competing with a strongly correlated traffic in the wireless segment, $y_1(t)$ has acquired a queuing behavior worse than that of $x_1(t)$. The contrary holds for $y_0(t)$, whose delay tail is significantly shorter than that of $x_0(t)$. It is interesting to note that the queuing behavior of $y_1(t)$ does not seem to be justified by the value of $\alpha_{OUT,1} = 0.01$ (Table 3). Such a value of $\alpha_{OUT,1}$ would suggest a slight deviation of the delay tail of $y_1(t)$ from that of $x_1(t)$. However, the deviation is large. We infer that $y_1(t)$ cannot be modeled simply as fGt.

In the one-hop scenario with different classes, a similar but milder phenomenon occurs: i.e., we still observe an increase of the delay tail of $y_1(t)$ and a decrease of the delay tail of $y_0(t)$, but the deviation of the delay tail of a traffic flow crossing the radio interface from that of the respective fresh input traffic flow is smaller. In this scenario, the isolation of service classes provided by the IEEE 802.11e EDCA seems to be effective.

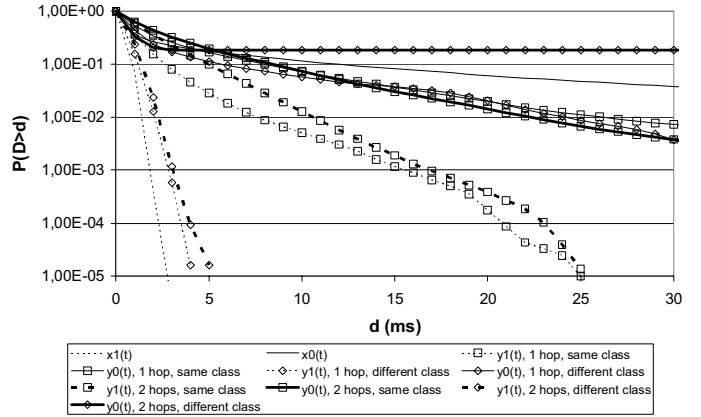


Fig. 11: delay behavior in the fixed network router R1, $\alpha_{IN,0}=0.8$, $\alpha_{IN,1}=0$.

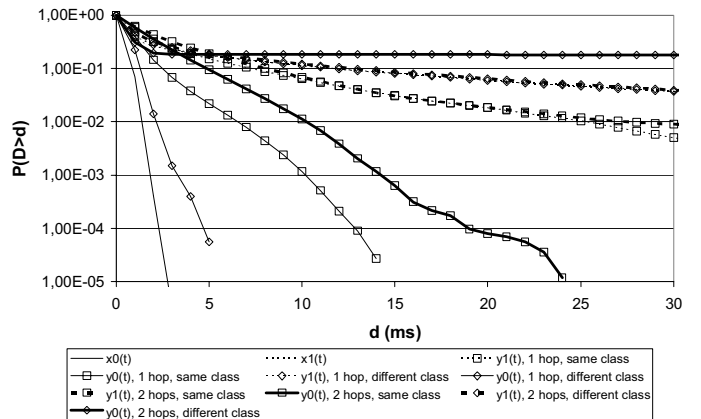


Fig. 12: delay behavior in the fixed network router R1, $\alpha_{IN,0}=0$, $\alpha_{IN,1}=0.8$.

With two wireless hops (scenario 2) and same class, the same basic considerations of the one-hop scenario and same class apply (the decrease of the delay tail of $y_0(t)$ is sharper). It is interesting to compare the behavior of $y_1(t)$ in this scenario and in the scenario with one hop and same class. In the two scenarios, the delay tails of $y_1(t)$ are very similar. However, the measured values of $\alpha_{OUT,1}$ (Table 3) would suggest the contrary, as with one hop $\alpha_{OUT,1} = 0.01$ and with two hops $\alpha_{OUT,1} = 0.39$. Also in this case, we infer that the statistical characterization of traffic changes deeply while crossing the IEEE 802.11e radio access network, in such a way that α is no longer sufficient to describe the queuing behavior of traffic. In the scenario with two wireless hops and different classes the isolation of flows provided by the IEEE 802.11 e EDCA function is rather effective, as the deviation of the delay tails of $y_1(t)$ and $y_0(t)$ from those of $x_1(t)$ and $x_0(t)$, respectively, are relatively small.

Fig. 12 refers to the same scenarios of Fig. 11, where the

priorities of $x_1(t)$ and $x_0(t)$ are exchanged. In this scenario, the white traffic has lower service priority and it is greatly affected by the competition with LRD traffic. It is particularly interesting the scenario with two wireless hops, where the flow $y_0(t)$ acquires a heavy tailed queuing behavior in the router R1 both in the same-class and different-class scenario. Remarkably, with different service classes, the originally white traffic acquires the fattest delay tail in R1. Moreover, with two hops and same class Table 3 reports that $\alpha_{OUT,1} = \alpha_{OUT,0} \sim 0.39$, therefore, we would expect a very similar delay tail for $y_1(t)$ and $y_0(t)$. Also in this case, our intuition is partially contradicted as even if both delay tails are fat, they are significantly different.

VI. CONCLUSIONS

We studied how traffic flows with different LRD parameters influence each other in IEEE 802.11e WLAN, in both one-hop and two-hop configurations. Our simulations account for the service class separation allowed by the IEEE 802.11e EDCA function and match results with those obtained in the basic scenario without separation of service classes.

In the scenarios selected, traffic flows, after having crossed the single-hop or two-hop radio interface, enter a fixed network node where they are served by a rate-based scheduler. In our work, we studied the LRD and queuing behavior of traffic at output of the wireless network.

As far as the LRD parameters of traffic are concerned, the analysis has shown that a strong mutual interference among flows occurs if a single service class is used, especially in the multi-hop scenario: i.e., the flow with smaller α parameter experiences an increase of α and the opposite holds for the flow with the larger α . Differentiating the service priorities by the mechanisms enabled by the IEEE 802.11e EDCA function improves significantly the isolation of service classes. However, in the multi-hop scenario this separation is partial.

In the second part of our analysis we studied the queuing behavior of the traffic output by the wireless network in the schedulers of a fixed network router. Since the queuing delay tail of LRD traffic is generally dominated by the α parameter, which determines how fat is the tail, we have tried to correlate delay tails with the corresponding α parameters of traffic measured at the output of the wireless network.

The results of the analysis are surprising, as the queuing behavior of traffic flows, after the crossing of the wireless segment, does not seem to depend on measured values of their α parameters. This observation hints that LRD traffic transported through the WLAN interface undergoes a deep structural change of its statistical model. A simple fGt model is not adequate to describe its behavior, at least as far as its queuing behavior is concerned.

REFERENCES

[1] W. E. Leland, M. S. Taqqu, W. Willinger, D. V. Wilson, "On the Self-Similar Nature of Ethernet Traffic (Extended Version)", *IEEE/ACM Transactions on Networking*, 2(1), February 1994.
 [2] V. Paxson, S. Floyd, "Wide Area Traffic: A Failure of Poisson Modeling", *IEEE/ACM Trans. on Networking*, 3(3), June 1995.

[3] M. Crovella, A. Bestavros. "Self-Similarity in World Wide Web Traffic: Evidence and Possible Causes", *IEEE/ACM Trans. on Networking*, 5(6), Dec. 1997.
 [4] J. Gao, R. Ritke, "Long-Range-Dependence and Multifractal Modeling of the vBNS Traffic", *Proc. of 2001 Applied Telecommun. Symp.*, Seattle, WA, USA, April 2001.
 [5] Qiong Li, David L. Mills, "On the Long-Range Dependence of Packet Round-trip Delays in Internet", *Proc. IEEE ICC 1998*, Atlanta, GA, USA, June 1998.
 [6] L. Guo, M. Crovella, I. Matta, "TCP Congestion Control and Heavy Tails", *Technical Report BU-CS-2000-017*, Boston Univ., July 2000.
 [7] J. M. Peha, "Retransmission Mechanisms and Self-Similar Traffic Models". *Proc. 1997 IEEE/ACM/SCS Commun. Netw. and Distr. Sys. Modeling and Simulation Conf.*, Phoenix, AZ, USA, January 1997.
 [8] A. Veres, B. Hungary, M. Boda, "The Chaotic Nature of TCP Congestion Control", *Proc. IEEE INFOCOM 2000*, Tel Aviv, Israel, Mar. 2000.
 [9] R. Ritke, X. Hong, M. Gerla, "Contradictory Relationship between Hurst Parameter and Queueing Performance (Extended Version)". *Telecommunications Systems*, 16(1,2) February 2001.
 [10] K. Park, W. Willinger, "Self-Similar Network Traffic: An Overview"; P. Abry, P. Flandrin, M. S. Taqqu, D. Veitch, "Wavelets for the Analysis, Estimation, and Synthesis of Scaling Data"; in *Self-Similar Network Traffic and Performance Evaluation*, K. Park, W. Willinger, Eds. Chichester, UK: John Wiley & Sons, 2000, pp. 1-88.
 [11] I. Norros, "A Storage Model with Self-similar Input", *Queueing systems*, 16 (1994), pp. 387-396.
 [12] D. P. Pazaros, M. Sifalakis, D. Hutchison, "On the Long-Range Dependent Behaviour of Unidirectional Packet Delay of Wireless Traffic", *Proc. IEEE Globecom 2007*, Washington, DC, USA, November 2007.
 [13] C. Oliveira, J. B. Kim, T. Suda, "Long-Range Dependence in IEEE 802.11b Wireless LAN Traffic: An Empirical Study", *Proc. IEEE 18th Annual Workshop on Comp. Commun.*, 20-21 October 2003.
 [14] Q. Liang, "Ad Hoc Wireless Network Traffic - Self-Similarity and Forecasting", *IEEE Comm. Letters*, vol. 6, n° 7, 297-299, July 2002.
 [15] J. Yu, A. Petropolu, "On Propagation of Self-Similar Traffic through an Energy-Conserving Wireless Gateway", *Proc. IEEE ICASSP 2005*, vol IV, 285-288.
 [16] O. Tickoo, B. Sikdar, "On the Impact of IEEE 802.11 MAC on Traffic Characteristics", *IEEE J. Select. Areas in Commun.*, vol. 21, n° 2, Feb. 2003, pp. 189-203.
 [17] C. Cano, D. Rincón, D. Remondo, "On the Mitigation of Long Range Dependence in IEEE 802.11", *Proc. 17th Annual IEEE Int. Symp. on PIMRC 2006*, Helsinki, Finland, 11-14 Sept. 2006.
 [18] IEEE 802.11e/D8.0, "Draft Amendment to Standard for Telecommunications and Information exchange between systems - LAN/MAN Specific Requirements - Part 11: Wireless Medium Access Control (MAC) and Physical Layer (PHY) Specifications: Medium Access Control (MAC) Quality of Service (QoS) Enhancements", Feb. 2004.
 [19] S. Bregni, L. Jmoda, "Accurate Estimation of the Hurst Parameter of Long-Range Dependent Traffic Using Modified Allan and Hadamard Variances", to appear in *IEEE Trans. Commun.*, 2008. Extended version available: <http://home.dei.polimi.it/bregni/public.htm>.
 [20] S. Bregni, P. Giacomazzi, G. Saddemi, "Output Traffic Characterization of Policers and Shapers with Long-Range Dependent Input Traffic", in *Proc. of IEEE GLOBECOM 2007*.
 [21] D. W. Allan, J. A. Barnes, "A Modified Allan Variance with Increased Oscillator Characterization Ability", *35th An. Freq. Contr. Symp.*, 1981.
 [22] P. Lesage, T. Ayi, "Characterization of Frequency Stability: Analysis of the Modified Allan Variance and Properties of Its Estimate", *IEEE Trans. Instrum. Meas.*, vol. 33, no. 4, pp. 332-336, Dec. 1984.
 [23] L. G. Bernier, "Theoretical Analysis of the Modified Allan Variance", *Proc. 41st Annual Freq. Contr. Symp.*, 1987.
 [24] S. Bregni, "Chapter 5 - Characterization and Modelling of Clocks", in *Synchronization of Digital Telecommunications Networks*. Chichester, UK: John Wiley & Sons, 2002, pp. 203-281.
 [25] S. Wietholter and C. Hoene, "Design and verification of an IEEE 802.11e EDCF simulation model in ns-2.26", *Proc. LCN 05*, <http://www.tkn.tuberlin.de/research/802.11e/ns2>.
 [26] I. Norros, "On The Use of Fractional Brownian Motion in the Theory of Connectionless Networks", *IEEE J. Select. Areas Commun.*, vol. 13, no. 6, pp. 953-962, Aug. 1995.